Article

Th(IV) Adsorption onto Oxidized Multi-Walled Carbon Nanotubes in the Presence of Hydroxylated Fullerene and Carboxylated Fullerene

Jing Wang [1], Peng Liu [1], Zhan Li [2], Wei Qi [1], Yan Lu [3], Wangsuo Wu [1],*

[1] Radiochemistry Laboratory, School of Nuclear Science and Technology, Lanzhou University, Lanzhou 730000, China; E-Mails: wangjing2010@lzu.edu.cn (J.W.); liupeng08@lzu.edu.cn (P.L.); qiwei20061987@126.com (W.Q.)

[2] Institute of Modern Physics, Chinese Academy of Sciences, Lanzhou 730000, China; E-Mail: lizhaner@126.com

[3] China National Nuclear Corporation Lanzhou Uranium Enrichment Co., Ltd., Lanzhou 730000, China; E-Mail: luyan08@lzu.edu.cn

* Author to whom correspondence should be addressed; E-Mail: wuws@lzu.edu.cn; Tel. / Fax: +86-093-1891-3594.

Abstract: The adsorption of Th(IV) onto the surface of oxidized multi-walled carbon nanotubes (oMWCNTs) in the absence and presence of hydroxylated fullerene ($C_{60}(OH)_n$) and carboxylated fullerene ($C_{60}(C(COOH)_2)_n$) has been investigated. $C_{60}(OH)_n$, $C_{60}(C(COOH)_2)_n$ and oMWCNTs have been chosen as model phases because of their representative in carbon nano-materials family. Adsorption experiments were performed by batch procedure as a function of contact time, pH, ionic strength, and temperature. The results demonstrated that the adsorption of Th(IV) was rapidly reached equilibrium and the kinetic process could be described by a pseudo-second-order rate model very well. Th(IV) adsorption on oMWCNTs was dependent on pH but independent on ionic strength. Adsorption isotherms were correlated better with the Langmuir model than with the Freundlich model. The thermodynamic parameters calculated from temperature-dependent adsorption isotherms suggested that Th(IV) adsorption on oMWCNTs was spontaneous and endothermic. Compared with the adsorption of Th(IV) on the same oMWCNTs free of $C_{60}(OH)_n$ or $C_{60}(C(COOH)_2)_n$, the study of a ternary system showed the inhibition effect of $C_{60}(OH)_n$ at high concentration on the adsorption of Th(IV) in a pH range from neutral to slightly alkaline; whereas the promotion effect of $C_{60}(C(COOH)_2)_n$, even at its low

concentration, on Th(IV) adsorption was observed in acid medium.

1. Introduction

Multiwalled carbon nanotubes (MWCNTs) have raised much interest during recent years due to their inherent extraordinary structural, mechanical, and electronic properties [1–3]. MWCNTs possess some highly desirable sorbent characteristics [4], which make them attractive for a variety of applications including radionuclide adsorption. Previous studies demonstrated that MWCNTs are the promising candidates in the field of chemical aspects of nuclear science and technology for the preconcentration and solidification of lanthanides and actinides from large volume of solutions [5–7]. Within the remarkable progress for industrial scale application, the toxicity of MWCNTs must be considered. Once they are released into the environment, the human health and environmental may suffer serious risks. CNTs can damage the plants, animals and human by entering the cells for their nanoscales [8–10]. The study showed that the toxicity of MWCNTs not only from itself but also from its adsorption substance. Therefore, understanding the adsorption of radionuclide on MWCNTs is crucial [11].

Thorium finds its extensive application as nuclear fuel in power plants and their main sources are soil, rocks, plants, sand and water. Nuclear spent fuels generally contain actinides like thorium, uranium and various fission products [12]. Th(IV) and its compounds are highly toxic that may cause acute toxicological effects for human leading to potential occupational carcinogens [13] and progressive or irreversible renal injury [14,15]. Thorium exists only stable as Th(IV) in solution, which is an important model element for other tetravalent actinides such as Np(IV), U(IV), and Pu(IV). It is also profit as a tracer for studying environmental important processes [16]. Based upon these importance of Th(IV), the determination of Th(IV) in environmental and biological samples is considerable potential as a tool for assessment of human exposure [15]. The fate and transport of Th(IV) in the environment is generally controlled by sorption reactions, complexation, colloid formation, *etc.* [17]. In recent years, the adsorption of Th(IV) on various materials has been studied extensively [18,19]. However, the adsorption behavior of actinide and lanthanide ions onto oMWCNTs is investigated in a limited number of studies [5–7,11,20,21], and the sorption mechanism is still unclear, especially in the presence of other nano-materials.

Fullerenes (C_{60}) is another kind of nanometer carbon materials whose discovery is earlier than carbon nanotubes. Due to its definite structure and π electron character, C_{60} is very easy to form π–π stacking interactions with another material equipped with aromatic rings [22,23], which may affect the adsorption of metal ions or organic matter on that material. Therefore, the research about the effect of fullerene on the adsorption of Th(IV) onto oMWCNTs is necessary. However, it is difficult to separate completely two kinds of carbon nano-materials in the identical phase, and to clarify their effect on the adsorptive interaction between carbon nano-materials and Th(IV). Herein, the author choose soluble fullerene to study its influence on the adsorption of Th(IV) onto oMWCNTs. It is essential to research

the adsorption of soluble fullerene and Th(IV) on oMWCNTs for understanding the radionuclide pollution and the potential impact evaluation of CNTs on radionuclide behavior.

2. Results and Discussion

2.1. Characterization of Purified oMWCNTs, $C_{60}(OH)_n$ and $C_{60}(C(COOH)_2)_n$

The transmission electron microscope (TEM, Hitachi Model H-600, Japan Hitachi company) was used to observe the changes in morphological features of oMWCNTs before and after two kinds of soluble fullerene adsorption. TEM image of oxidized MWCNTs (Figure 1a) display that carbon nanotubes have smooth surface and integrated hollow tubular structure. It can be seen from Figure 1b that $C_{60}(OH)_n$ particles (see the narrow present) spread heterogeneously on the surface of oMWCNTs for the $C_{60}(OH)_n$-adsorbed oMWCNTs. Figure 1c indicates that $C_{60}(C(COOH)_2)_n$ particles does not attach with oMWCNTs.

Figure 1. Transmission electron microscope (TEM) images of (**a**) oxidized multi-walled carbon nanotubes (oMWCNTs); (**b**) $C_{60}(OH)_n$-adsorbed oMWCNTs; (**c**) $C_{60}(C(COOH)_2)_n$-adsorbed oMWCNTs.
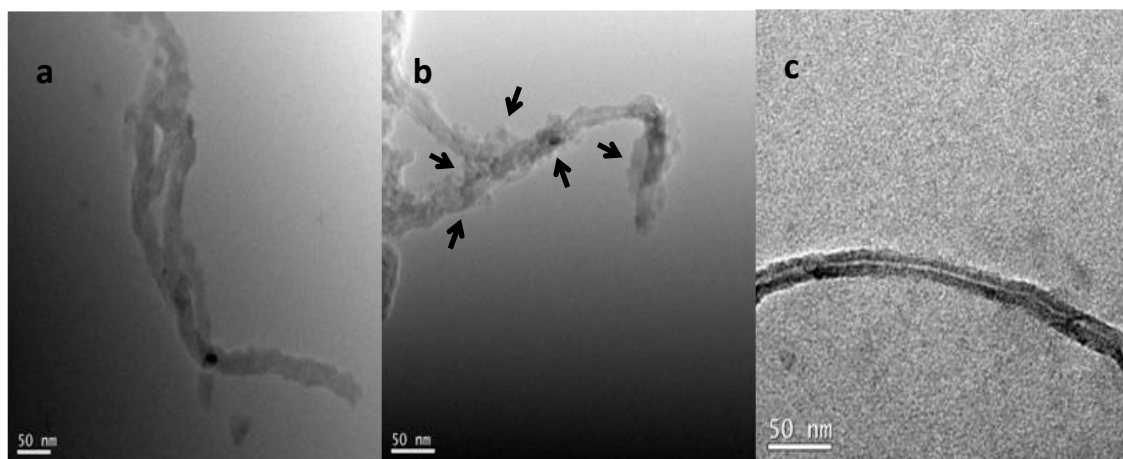
Fourier transform infrared (FTIR, Nexus670, Thermo Nicolet, American) technique was used in the analysis of the chemical surface groups of the adsorbents. Figure 2 illustrates the FT-IR spectrum of the oxidized carbon nanotubes. The peak at 3440 cm^{-1} is attributed to –OH stretching mode. The peaks at 2918 and 2849 cm^{-1} assigned to asymmetric and symmetric –CH stretching bands. The C=O stretching vibrations peak are appeared at 1710 cm^{-1}. The peak at 1625 and 1436 cm^{-1} assigned to C=C stretching bands. The peak at 1513 cm^{-1} can be attributed the carboxylic and carboxylate anion stretching mode. The peak between 1100 and 1376 cm^{-1} is associated with C–O stretching and –OH bending modes of alcoholic, phenolic and carboxylic groups [24,25].

Figure 3 shows the FT-IR spectrum of raw C_{60}, $C_{60}(OH)_n$ and $C_{60}(C(COOH)_2)_n$. For $C_{60}(OH)_n$ (Figure 3b), the FTIR spectrum exhibit main peaks at wavenumbers near 3234, 1609, 1365 and 1086 cm^{-1}, which are associated with –OH, C=C and –C–O groups [26]. The bands at wavenumbers of 3439, 1718, 1201 and 523 cm^{-1} for $C_{60}(C(COOH)_2)_n$ (Figure 3c) are indicative of the appearance of the stretching of hydroxyl (–OH), carbonyl (>C=O) and carboxyl (–C–O) groups, respectively [27].

Figure 2. Fourier transform infrared (FTIR) spectra of oMWCNTs.
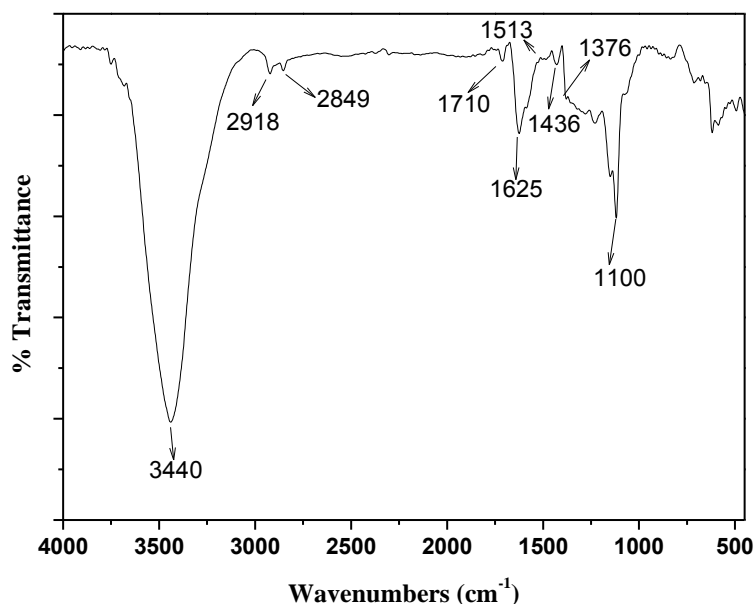
Figure 3. FTIR spectra of the samples: (**a**) raw C_{60}; (**b**) $C_{60}(OH)_n$; (**c**) $C_{60}(C(COOH)_2)_n$.
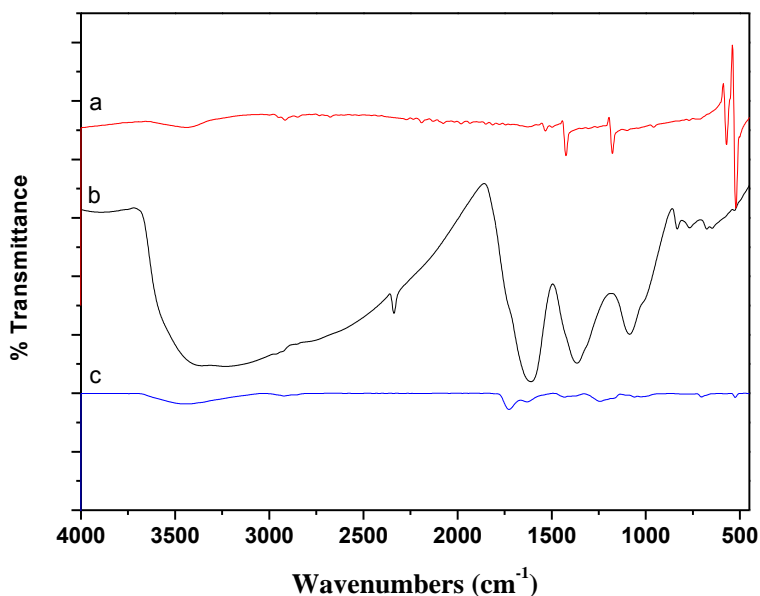
2.2. Adsorption of Th(IV) onto oMWNTs Surface

2.2.1. The Sorption Kinetics

The influence of contact time on the Th(IV) adsorption by oMWNTs was studied. The initial Th(IV) concentrations was 8.86×10^{-5} mol/L in the kinetic study. As seen from Figure 4, the uptake of Th(IV) onto oMWCNTs is rapid at the initial contact time, and then the adsorption equilibrium is reached within 3 h. The quick adsorption of Th(IV) suggests that chemical adsorption rather than physical adsorption contributes to Th(IV) adsorption onto oMWCNTs surface [28]. To analyze the adsorption rate of Th(IV) onto oMWCNTs, the pseudo-second-order rate equation (Equation (1)) [29] is employed to simulate the kinetic adsorption data. Its general form is

$$\frac{t}{q_t} = \frac{1}{k_0 q_e^2} + \frac{t}{q_e} \tag{1}$$

where q_t (mg/g) is the amount of Th(IV) adsorbed on oMWCNTs at time t and q_e (mg/g) is the equilibrium sorption capacity. k_o (g/mg·h^{-1}) is the pseudo-second-order rate constant of sorption. The straight-line plots of t/q_t *vs.* t (Figure4) is plotted and values of k_o (1.81 × 10^{-3} g/mg·h^{-1}) and q_e (6.44 × 10^{-3} mg/g) are calculated from the intercept and slope of Equation (1). The correlation coefficient of the pseudo-second-order rate equation for the linear plot is 0.9999, which suggests that the kinetic sorption can be described by the pseudo-second-order rate equation very well. Based on the above results, an equilibrium time is selected as 24 h for all subsequent batch experiments.

Figure 4. Effect of contact time on Th(IV) adsorption rate onto oMWCNTs and test of pseudo-second-order adsorption kinetics plot for Th(IV), *m/V* = 0.1 g/L, *T* = 25 ± 1 ℃, C[Th^{4+}] initial = 8.86 × 10^{-5} mol/L, *I* = 0.01 mol/L NaNO$_3$, pH = 3.20 ± 0.05.
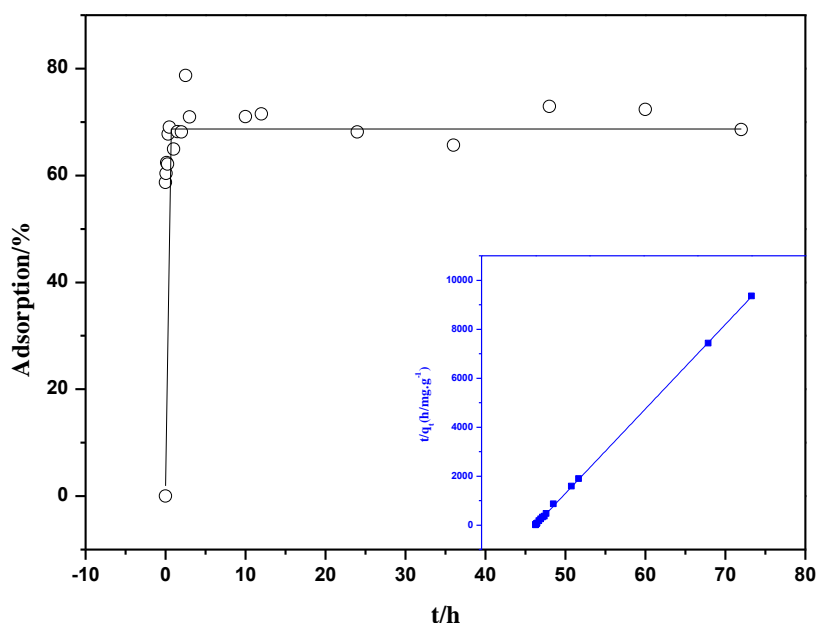
2.2.2. Influence of pH and Ionic Strength

The pH of solution is a controlling factor in Th(IV) adsorption experiments. Figure 5 shows the effect of pH on Th(IV) removal by varying the pH from1 to 10 in 0.001, 0.01 and 0.1 mol·L^{-1} NaNO$_3$ solution. As shown in Figure 5, Th(IV) adsorption is strongly influenced by the solution pH values. As pH increased from 1 to 4, the fraction of Th(IV) adsorbed onto oMWCNTs also increased, and then the adsorption of Th(IV) maintains at the maximum value of 92% after pH ≥ 4. The maximum adsorption in the pH range 3–4 may be due to the formation of Th(IV) complexes with carboxyl groups on the surface of oMWCNTs. It is well known that oxidation of carbon surface can offer not only more hydrophilic surface structure, but also a large number of oxygen-containing functional groups like –COOH, –OH, or –C=O on the surfaces of oMWCNTs, which increase the sorption capability of carbon material [5]. The results are similar to the Th(IV) adsorption on anatase [30] and silica [31]. The increase of Th(IV) adsorption on oMWCNTs with increasing of pH may be attributed to the

surface properties of oMWCNTs in terms of surface charge and dissociation of functional groups [32]. The surface of oMWCNTs contains a large number of binding sites, which may become positively charged at low pH due to the protonation reaction on the surfaces (*i.e.*, $SOH + H^+ \Leftrightarrow SOH_2^+$). The point of zero charge (pH_{pzc}) of oMWCNTs is about 5 [6,33]. At pH < 5, the surfaces were positively charged, and at pH > 5, the surface were negatively charged. The electrostatic repulsion occurred between Th(IV) and the edge groups with positive charge (SOH_2^+) on oMWCNTs surface results in the low adsorption efficiency of Th(IV). At high pH values, the surface of oMWCNTs becomes negatively charged due to the deprotonation process (*i.e.*, $SOH \Leftrightarrow SO^- + H^+$) and electrostatic repulsion decreases with increasing of pH because of the reduction of positive charge density on the adsorption edges, which enhances the adsorption of the positively charged Th(IV) ions through electrostatic attraction. The characteristic of Th(IV) complex that predominates at a specific solution pH may also play an important role in the uptake efficiency of oMWCNTs for Th(IV) adsorption [34]. According to the hydrolysis constants of Th(IV) ($\log k_1 = -3.86$, $\log k_2 = -11.82$, $\log k_3 = -24.81$, $\log k_4 = -41.97$) [35,36], Th(IV) species present in the forms of Th^{4+}, $Th(OH)^{3+}$, $Th(OH)_2^{2+}$, $Th(OH)_3^{3+}$, $Th(OH)_4$ at different pH values. As can be seen from Figure 5, it is clear that Th(IV) starts to form precipitation at pH = 3.85 if no Th(IV) is adsorbed on oMWCNTs. However, one can see that more than 90% Th(IV) has been adsorbed onto oMWCNTs at pH < 3.85. Therefore, the abrupt increasing of Th(IV) adsorption is not attributed to the precipitation of $Th(OH)_4(s)$. Sheng *et al.* [37] studied the adsorption of Th(IV) on alumina and they did not think the precipitation is the removal mechanism of alumina toward Th(IV) at pH < 4. They pointed out that the high adsorption of Th(IV) on the surface of oMWCNTs may result in the precipitation of Th(IV) on oMWCNTs due to the local high concentration of Th(IV) on oMWCNTs surface [38,39].

Figure 5. Adsorption of Th(IV) on oMWCNTs as a function of pH, *m/V* = 0.1 g/L, *T* = 25 ±1 ℃, C[Th^{4+}] initial = 8.86×10^{-5} mol/L.
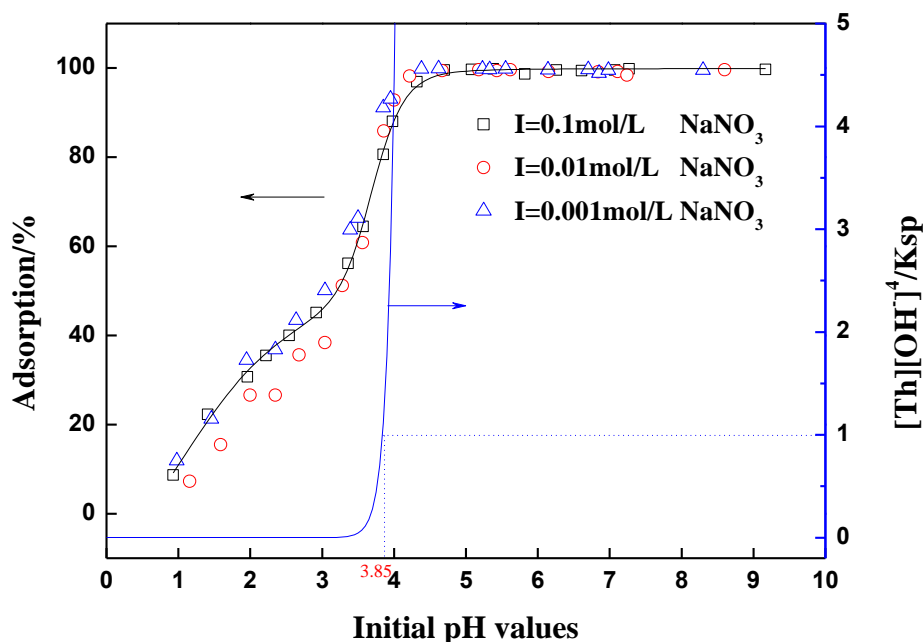
Figure 5 also shows the adsorption of Th(IV) onto oMWCNTs as a function of ionic strength at pH 1–10. Th(IV) adsorption is independent of the ionic strength, which suggests that inner-sphere surface complexes has been formed under this experimental condition [6,11]. Therein, ion exchange does not contribute to the adsorption of Th(IV) onto oMWCNTs. In general, strong dependency on pH and weak dependency on ionic strength, are consistent with inner-sphere complexation [40]. The results of this work are identical to those derived from the literature [12,13,41], although different adsorbate or adsorbents are investigated in the present work.

2.2.3. Influence of the Concentration of oMWCNTs

Adsorption of Th(IV) as a function of oMWCNTs content is shown in Figure 6. The distribution coefficient (K_d) was calculated from the initial concentration of Th(IV) (C_0) and the equilibrium one (C_e) according to the following equation:

$$k_d = \frac{C_0 - C_e}{C_0} \times \frac{V}{m}$$

(2)

where V is the volume of the solution and m is the mass of oMWNCTs. One can see that the sorption percentage of Th(IV) increases with increasing content of oMWCNTs in the system. The functional sites on oMWCNTs surfaces increase with increasing of oMWCNTs content, therefore the sorption percentage of Th(IV) increases reasonably. However, the K_d value increases slightly with increasing content of oMWCNTs. The results of this work are very similar to the literature [42].

Figure 6. Effect of solid content on the adsorption of Th(IV) onto oMWCNTs, pH = 3.20 ± 0.05, T = 25 ± 1 ℃, C[Th^{4+}] initial = 8.86 × 10^{-5} mol/L, I = 0.01 mol/L NaNO$_3$.
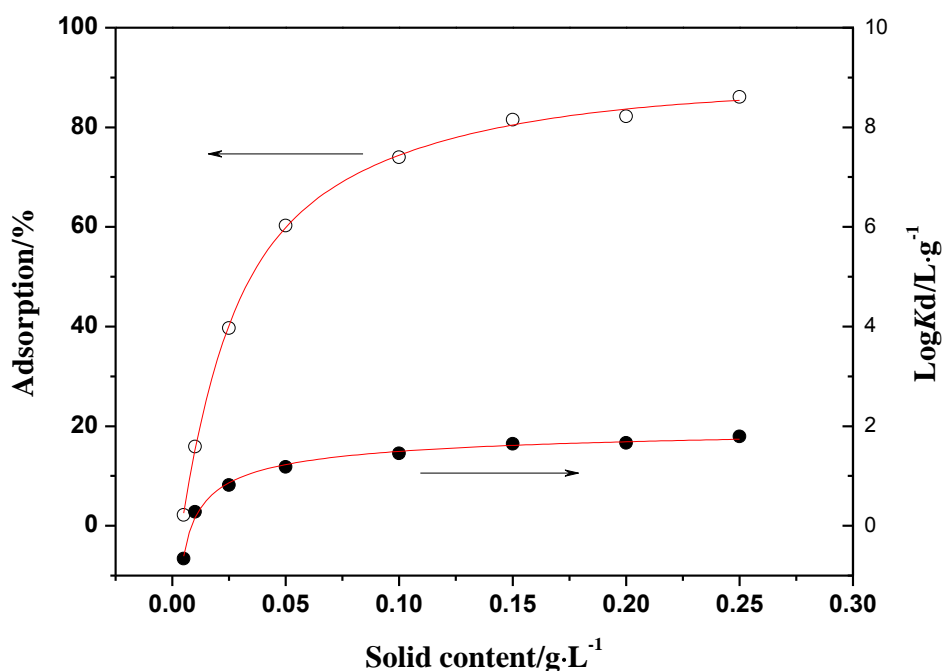
2.2.4. Adsorption Isotherms

The effect of temperature on the adsorption of Th(IV) was studied by performing a series of experiments at 298, 318 and 338 K. The concentration of Th(IV) varied from 0 to 8.86×10^{-4} mol/L. Figure 7 shows the Th(IV) adsorption isotherm on oMWCNTs. The Langmuir model and Freundlich model were used to analyze regressively the adsorption isotherms of Th(IV). The linear form of the Langmuir model can be represented by the following equation:

$$\frac{C_e}{q_e} = \frac{1}{K_L q_{max}} + \frac{C_e}{q_{max}} \qquad (3)$$

where q_e (mg/g) and C_e (mg/L) are respectively for the concentration of the metal ions in the solid and liquid phases in equilibrium adsorption, K_L (L/g) is the adsorption equilibrium constant, q_{max} (mg/g) is the maximum adsorption capacity of the metal ion.

The Freundlich isotherm has the following linear form:

$$\log q_e = \log K_F + n \log C_e \qquad (4)$$

where q_e (mg/g) represents the adsorption amount of the metal ions in the unit mass of oMWCNTs; C_e (mg/L) is the equilibrium aqueous concentration; K_F and n are the absorption capacity and strength in the Freundlich the equilibrium constants, respectively.

Figure 7. Adsorption isotherms of Th(IV) on oMWCNTs at three different temperatures, $m/V = 0.1$ g/L, pH $= 3.20 \pm 0.05$, $I = 0.01$ mol/L NaNO$_3$, C[Th^{4+}] initial $= 8.86 \times 10^{-5}$ mol/L.
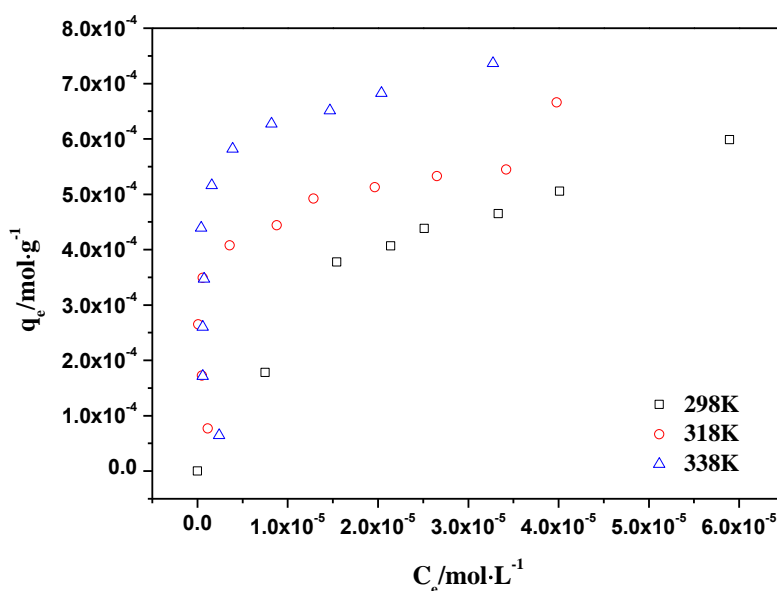
The linearized Langmuir and Freundlich plots are shown in Figures 8 and 9. Parameter values for two kinds of models are presented in Table 1. The Langmuir model showed a higher correlation coefficient than the Freundlich model. This is consistent with the results in the literature, which shows that the adsorption of Th(IV) on the other materials meet the Langmuir model better [43]. The thermodynamic parameters of ΔH^0, ΔG^0 and ΔS^0 calculated from different adsorption isotherms are tabulated in Table 2. The ΔH^0 value was positive as expected for an endothermic reaction under the

conditions applied. Figure 7 also confirmed that the adsorption of Th(IV) on oMWCNTs increases with increasing temperature. The negative ΔG^0 value indicated that the adsorption process is spontaneous for Th(IV) adsorption. The decrease in ΔG^0 with the increase of temperature exhibited more efficient adsorption at higher temperature [5].

Figure 8. Langmuir model of Th(IV) adsorption onto oMWCNTs, $m/V = 0.1$ g/L, pH = 3.20 ± 0.05, $I = 0.01$ mol/L NaNO$_3$, C[Th^{4+}] initial $= 8.86 \times 10^{-5}$ mol/L.
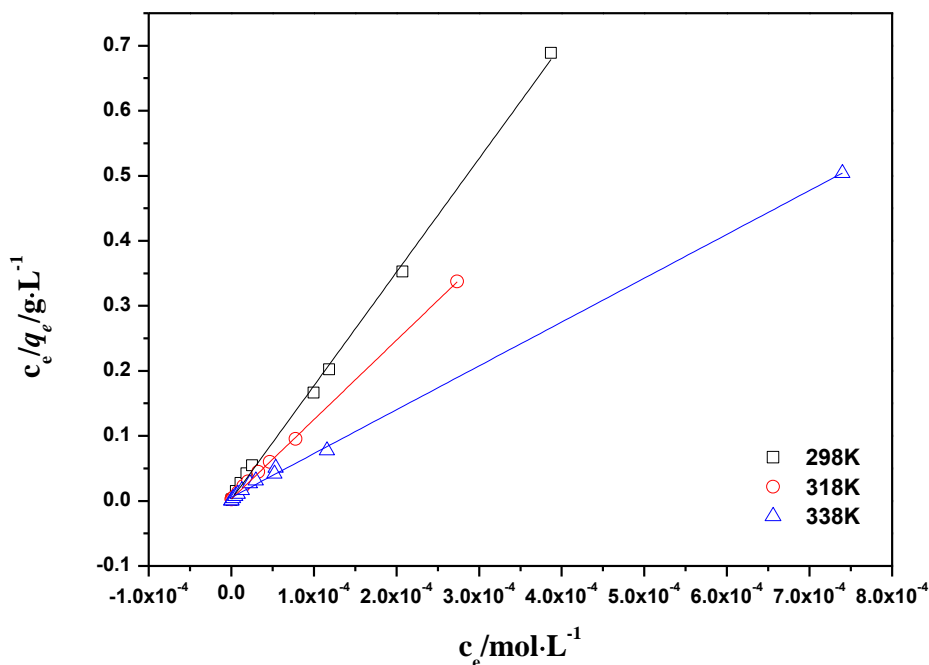
Figure 9. Freundlich model of Th(IV) adsorption onto oMWCNTs, $m/V = 0.1$ g/L, pH = 3.20 ± 0.05, $I = 0.01$ mol/L NaNO$_3$, C[Th^{4+}] initial $= 8.86 \times 10^{-5}$ mol/L.
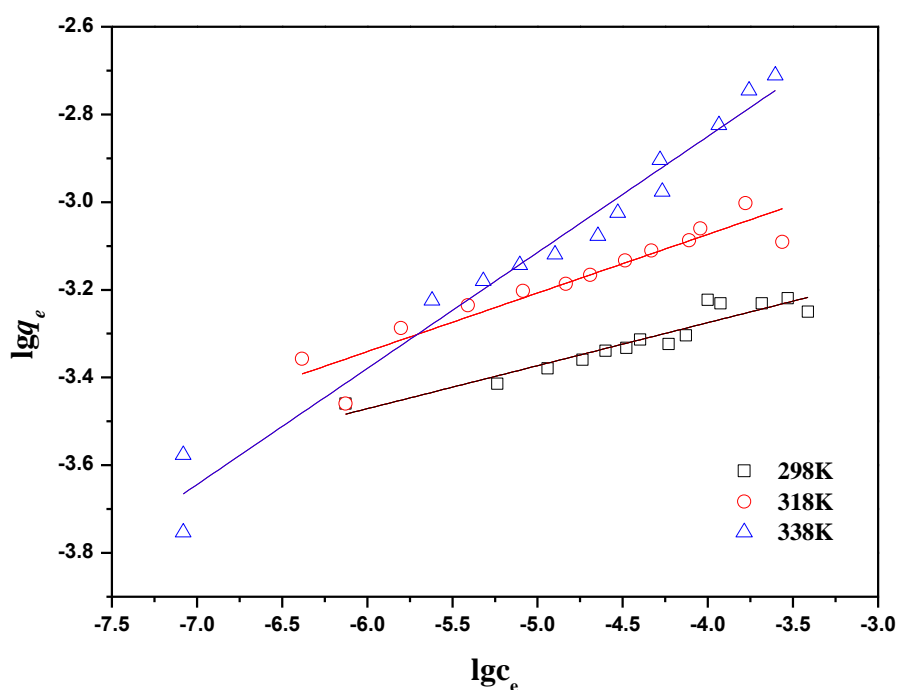
Table 1. The parameters of Langmuir and Freundlich fitting of Th(IV) adsorption on oMWCNTs.

T(K)	Langmuir constants			Freundlich constants		
	q_{max} (mg g^{-1})	K_L	R^2	K_F (mg^{1-n} L^n g^{-1})	n	R^2
298	5.72×10^{-4}	423.7	0.998	1.31×10^{-3}	0.09	0.887
318	8.18×10^{-4}	359.7	0.999	2.89×10^{-3}	0.13	0.881
338	1.48×10^{-3}	185.2	0.998	1.62×10^{-3}	0.26	0.969

Table 2. Values of thermodynamic parameters for the adsorption of Th(IV) on oMWCNTs.

C_0 (mg L^{-1})	ΔH^0 (KJ mol^{-1})	ΔS^0 (J mol^{-1} K^{-1})	ΔG^0 (KJ mol^{-1})		
			298 K	318 K	338 K
7.09×10^{-5}	42.65	168.12	−7.19	−11.47	−13.84
7.98×10^{-5}	39.52	154.88	−6.53	−10.03	−12.69
8.87×10^{-5}	33.67	134.09	−6.17	−9.28	−11.51
1.06×10^{-4}	32.15	125.75	−5.17	−8.23	−10.15

2.3. Influence of $C_{60}(OH)_n$ on the Adsorption of Th(IV)

2.3.1. Adsorption of Th(IV) *vs.* pH in the Presence of $C_{60}(OH)_n$

Figure10 presents Th(IV) adsorption onto oMWCNTs in the absence and presence of $C_{60}(OH)_n$ as a function of pH values. The concentration of $C_{60}(OH)_n$ is fixed from 10 to 250 mg/L. The adsorption curve of Th(IV) in ternary system presented in Figure 10 can be divided into two different parts. Within the first region ($1 \leq pH \leq 4$), the adsorption of Th(IV) increases with increasing pH in the presence of $C_{60}(OH)_n$. However, the adsorption hindrance of Th(IV) appears in the presence of high concentration of $C_{60}(OH)_n$ (*i.e.*, 125 and 250 mg/L) at pH 4. The second region lies where the adsorption of Th(IV) markedly decreases with increasing pH when pH exceeds 4 in ternary system. A striking observation can be made that the decreases of Th(IV) adsorption is correlated strongly to the concentration of $C_{60}(OH)_n$. The adsorption curve of Th(IV) in the presence of 10 mg/L $C_{60}(OH)_n$ is similar to that in the absence of $C_{60}(OH)_n$. When the concentration of $C_{60}(OH)_n$ is 125 mg/L, the adsorption of Th(IV) decreases from approximate 83% at pH 4 to 20% at pH 8.5. While the adsorption of Th(IV) decreases from nearly 63% at pH 4 to 3% at pH 8.5 when 250 mg/L $C_{60}(OH)_n$ is added. It can be stated that $C_{60}(OH)_n$ impedes obviously the adsorption of Th(IV) onto oMWCNTs. These observations are not in agreement with the general behavior of Th(IV) in natural systems, which are associated with organic matter [17,44–46].

The decreases of Th(IV) adsorption on oMWCNTs may be explained by a competition between $C_{60}(OH)_n$ and Th(IV) for the sorption sites on the oMWCNTs surface. Both the adsorption of Th(IV) and $C_{60}(OH)_n$ occurred on the surface of oMWCNTs, whereas Th(IV) cannot interact with $C_{60}(OH)_n$. In other words, $C_{60}(OH)_n$-oMWCNTs and Th-oMWCNTs complexes can be formed but $C_{60}(OH)_n$-Th may not formed. Figure 1B confirms that the adsorption of $C_{60}(OH)_n$ takes place onto oMWCNTs. Figure A1 demonstrates that the zeta potential of oMWCNTs in solution decreases regularly with increasing concentration of $C_{60}(OH)_n$. This verified that the dispersivity of oMWCNTs in solution has been improved by adsorbed $C_{60}(OH)_n$. The adsorption of $C_{60}(OH)_n$ on oMWCNTs depends on the strong π–π electron donor-acceptor interactions between the flat surfaces of both aromatic $C_{60}(OH)_n$

and oMWCNTs [47]. The complexation between $C_{60}(OH)_n$ and oMWCNTs is stronger than that between Th(IV) and oMWCNTs. Adsorbed $C_{60}(OH)_n$ may block available sites of oMWCNTs surface which would be originally for the adsorption of Th(IV) [31]. With increasing pH, Th(IV) would be "squeezed" down by the increasing adsorption of $C_{60}(OH)_n$ on oMWCNTs due to the enhancement of space hindrance.

Figure 10. Effect of $C_{60}(OH)_n$ on Th(IV) adsorption onto oMWCNTs as a function of pH, $m/V = 0.1$ g/L, $T = 25 \pm 1$ ℃, $I = 0.01$ mol/L $NaNO_3$, C[Th^{4+}] initial = 8.86×10^{-5} mol/L.
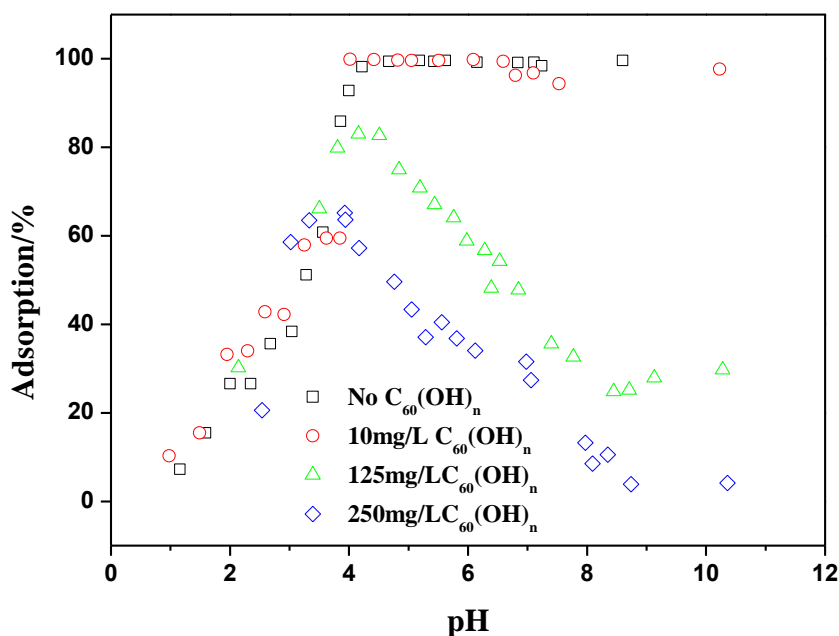
From Figure 10, one can still see that at pH > 9, Th(IV) adsorption rises again slightly, which could be due to following factors: at pH > 9, $Th(OH)_3(CO_3)^-$ and $Th(CO_3)_5^{6-}$ is expected to begin forming and $Th(OH)_4$ is the predominating species. Adsorbed $C_{60}(OH)_n$ on oMWCNTs surface enhances electrostatic repulsion of the $Th(OH)_3(CO_3)^-$ and $Th(CO_3)_5^{6-}$ [31]. In general, the adsorption behavior of Th(IV) in the presence of $C_{60}(OH)_n$ may be described as a competition between Th(IV) and $C_{60}(OH)_n$ for the binding sites on the surface of oMWCNTs. Adsorbed $C_{60}(OH)_n$ may also affect the adsorption of Th(IV) by altering surface charges and/or blocking available sites binding Th(IV). This assumption was not verified, and further work is in progress.

2.3.2. Adsorption Isotherms at Constant Adsorbent Dose and Initial Concentration

Adsorption experiments have been conducted at constant concentrations of Th(IV) and ratio of solid to liquid as a function of $C_{60}(OH)_n$ concentration (as shown in Figures 11 and 12). The $C_{60}(OH)_n$ concentration varied from 0 to 250 mg/L. In a general manner, Th(IV) adsorption onto oMWCNTs decreases when $C_{60}(OH)_n$ concentration increases whatever the concentrations of Th(IV) and ratio of solid to liquid is. The adsorption isotherms reveals a similar behavior as can be seen from Figures 10 and 11 shows that Th(IV) adsorption decreases by half with the initial concentration of Th(IV) decreasing by half, indicating that Th(IV) does not interact with $C_{60}(OH)_n$. Figure 12 presents that when the dosage of oMWCNTs are 0.2 and 0.1 g/L and the concentration of $C_{60}(OH)_n$ is less than

100 mg/L, the adsorption of Th(IV) on oMWCNTs maintains stable at a high level, then falls sharply when the concentration of $C_{60}(OH)_n$ exceeds 100 mg/L. As the dosage of oMWCNTs is 0.05 g/L, Th(IV) adsorption decreases gradually when the concentration of $C_{60}(OH)_n$ is more than 100 mg/L and remains at a minimum value of ~25%. This may be demonstrates indirectly the adsorption of $C_{60}(OH)_n$ on oMWCNTs.

Figure 11. Effect of Th(IV) initial concentrations on Th(IV) adsorption onto oMWCNTs as a function of $C_{60}(OH)_n$ initial concentrations, $m/V = 0.1$ g/L, pH = 3.20 ± 0.05, $I = 0.01$ mol/L NaNO$_3$, $T = 25 \pm 1$ ℃.
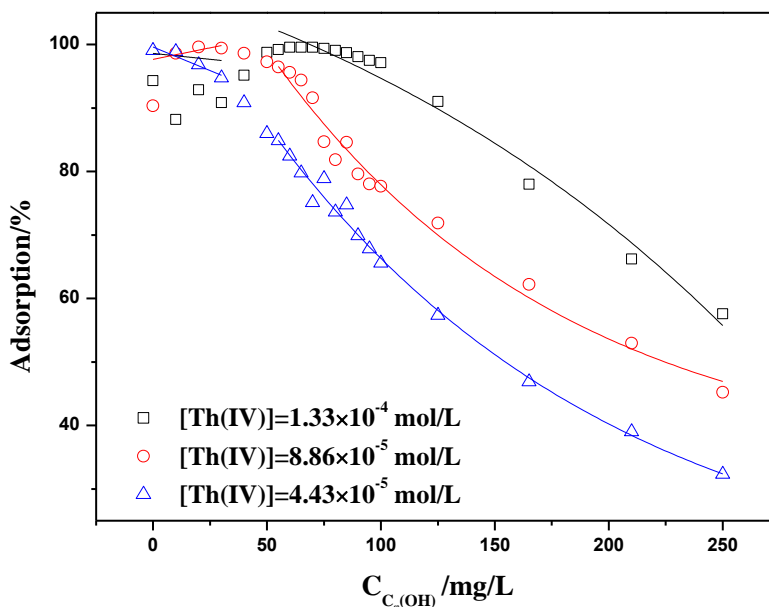
Figure 12. Effect of oMWCNT dosage on Th(IV) adsorption on oMWCNTs as a function of $C_{60}(OH)_n$ initial concentrations, pH = 3.20 ± 0.05, $I = 0.01$ mol/L NaNO$_3$, $T = 25 \pm 1$ ℃, C[Th^{4+}] initial = 8.86×10^{-5} mg/L.
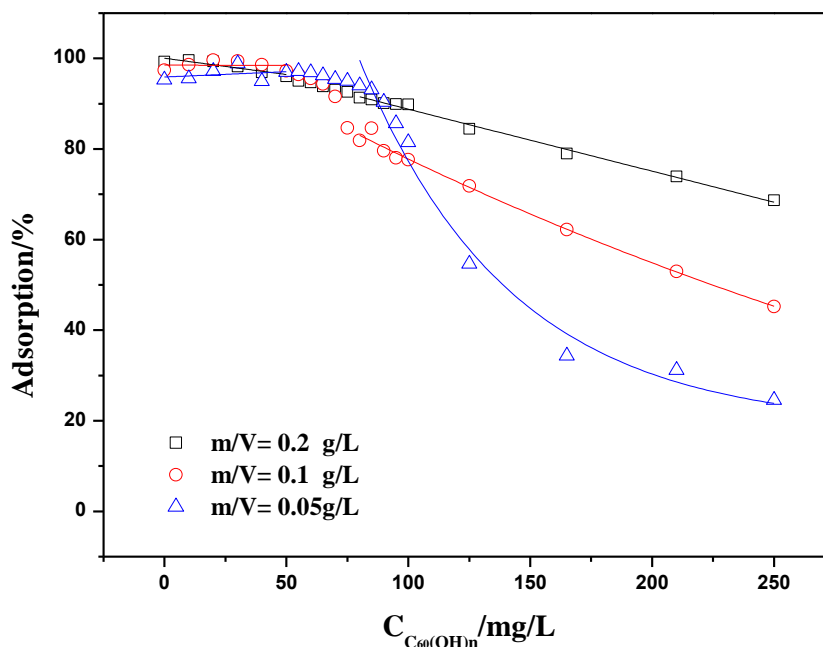
Both of the experimental curves in Figures 11 and 12 can be divided into two distinct regions. In the first region, where the concentration of $C_{60}(OH)_n$ is lower than 50 mg/L, Th(IV) adsorption is more than 90%; In the second region, where the concentration of $C_{60}(OH)_n$ is higher than 50 mg/L, the adsorption of Th(IV) onto oMWCNTs is decreased with increasing $C_{60}(OH)_n$ concentration. That is to say, $C_{60}(OH)_n$ suppresses the Th(IV) adsorption when its concentration exceeds a critical value.

2.4. Influence of $C_{60}(C(COOH)_2)_n$ on Th(IV) Adsorption

Figure 13 exhibits the adsorption of Th(IV) on oMWCNTs as a function pH in the presence and absence of $C_{60}(C(COOH)_2)_n$. The adsorption curve of Th(IV) onto oMWCNTs in the presence of $C_{60}(C(COOH)_2)_n$ shifts to the left as compared to that in the absence of $C_{60}(C(COOH)_2)_n$ at pH < 4, from which it can be concluded that the presence of $C_{60}(C(COOH)_2)_n$ enhances Th(IV) adsorption at pH < 4. Moreover, the adsorption of Th(IV) increases with increasing of $C_{60}(C(COOH)_2)_n$ concentration. It can conjectured that the complexation between $C_{60}(C(COOH)_2)_n$ and Th(IV) is formed. The complexes may promote the precipitation of Th(IV) on the surface of oMWCNTs [37]. Therefore Th(IV) adsorption on oMWCNTs is enhanced in the presence of $C_{60}(C(COOH)_2)_n$ in ternary system. But with increasing of pH, one can see that Th(IV) adsorption reduces slightly at intermediate pH (~4–6) and then rises again until equilibrium at pH > 6. This also indicates that the negative effect of $C_{60}(C(COOH)_2)_n$ on Th(IV) sorption is different from that of $C_{60}(OH)_n$. The steric hindered effect of $C_{60}(C(COOH)_2)_n$ is stronger than that of $C_{60}(OH)_n$, and $C_{60}(C(COOH)_2)_n$ can not easily be adsorbed onto oMWCNTs like $C_{60}(OH)_n$. This may be the reason why no $C_{60}(C(COOH)_2)_n$ connected to oMWCNTs surface is observed in the TEM photos of the dispersion of oMWCNTs and $C_{60}(C(COOH)_2)_n$ (seen from Figure 1C). However, $C_{60}(C(COOH)_2)_n$ can adsorbed on oMWCNTs surface due to the interaction of their functional groups at intermediate pH, which results in the increasing space hindrance of $C_{60}(C(COOH)_2)_n$, thus reducing the Th(IV)adsorption.

Figure 13. Effect of $C_{60}(C(COOH)_2)_n$ on Th(IV) adsorption onto oMWCNTs as a function of pH, $m/V = 0.1$ g/L, $T = 25 \pm 1$ ℃, $I = 0.01$ mol/L NaNO$_3$, C[Th^{4+}] initial $= 8.86 \times 10^{-5}$ mol/L.
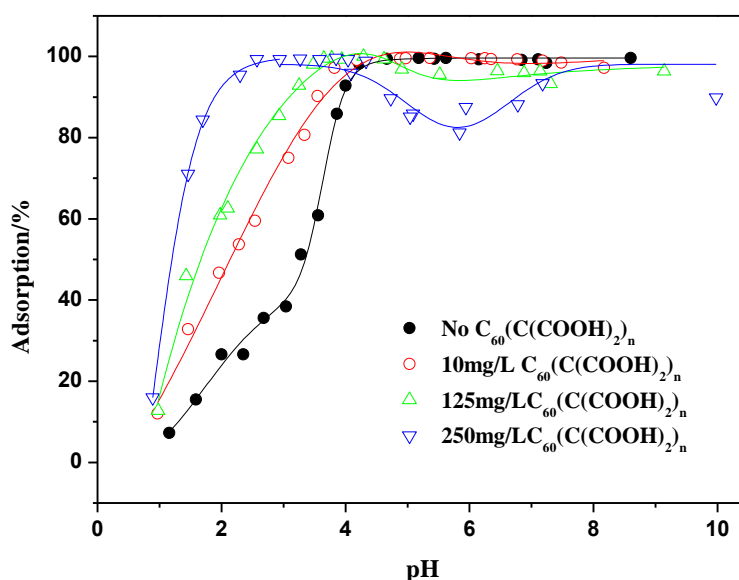
3. Experimental Section

3.1. Materials

MWCNTs (prepared by chemical vaporization deposition) were purchased from Shenzhen Nanotech Port Co., Ltd. China. According to the product specification, the as-grown MWCNTs are 1−10 μm in length, with outer diameter range of 10−30 nm, and purity above 96% (including amorphous carbon < 3%, ash < 0.2%). Oxidized MWCNTs were prepared by oxidization with a mixture of concentrated nitric acid and sulfuric acid (1:3, V/V) [48]. The surface area of oMWCNTs is 100 m^2/g determined using N_2-BET method (micromeritics Surface Area and Porosity Analyzer, ASAP 2020, American). Chen *et al.* [49] have measured the surface area of raw carbon nanotubes and the result was 86 m^2/g. This indicates that the oxidation process improves the specific surface area of the MWCNTs.

Fullerenes (C_{60}), purity > 99%, was bought from Henan Puyang Yongxin Fullerene Technology Co., LTD. $C_{60}(OH)_n$ ($n = 2\sim24$) was synthesized in the procedure reported by Li *et al.* [50]. Synthesis of $C_{60}(C(COOH)_2)_n$ has been described in the literature [51].

All chemicals were of analytical grade and all solutions were prepared using deionized water.

3.2. Adsorption Experiments

The adsorption of Th(IV) on oMWCNTs was investigated using batch technique in 10 mL polyethylene centrifuge tube. The stock solutions of oMWCNTs and $NaNO_3$ were mixed and pre-equilibrated for 24 h and then the Th(IV) stock solution was added to achieve the desired concentrations of different components. The system was adjusted to the desired pH by adding negligible volumes of 0.01 or 0.1 mol L^{-1} HNO_3 or NaOH. After the suspensions were gently shaken for 24 h (which was enough to achieve equilibrium), the solid and liquid phases were separated by using centrifugating at 12,000 rpm for 30 min. The concentration of Th(IV) in the aqueous solution was analyzed using the thorium arsenazo(III) complex method with UV-VIS spectrophotometer (Perkin-Elmer, American) at 654 nm. The amount of Th(IV) adsorption was calculated from the difference between the initial concentration and the equilibrium one.

Adsorption isotherms were investigated by using batch technique in polyethylene centrifuge tubes under ambient conditions at 293, 313, and 333 K, respectively. The stock solutions of 0.01 mol/L $NaNO_3$ and 0.5 g/L oMWCNTs were mixed and pre-equilibrated for 24 h before the addition of Th(IV) stock solution. The initial concentrations of Th(IV) varied from 8.86×10^{-6} to 8.86×10^{-4} mol/L.

The effect of $C_{60}(OH)_n$/$C_{60}(C(COOH)_2)_n$ on the adsorption of Th(IV) was also investigated. The stock solutions of oMWCNTs and $C_{60}(OH)_n$/$C_{60}(C(COOH)_2)_n$ and $NaNO_3$ were mixed and pre-equilibrated for 24 h before adding the Th(IV) stock solution. Other procedures were the same as the single-solute sorption experiments.

4. Conclusions

The results of the present work indicated that chemical complexation was the main mechanism of Th(IV) adsorption onto oMWCNTs. The competition adsorption between $C_{60}(OH)_n$ and Th(IV) may

be attributed to the negative effects of $C_{60}(OH)_n$ on Th(IV) adsorption onto oMWCNTs. While $C_{60}(C(COOH)_2)_n$ exhibited positive effect may be due to the fact that $C_{60}(C(COOH)_2)_n$ promoted the precipitation of Th(IV). The results are important to understand the fate and transport of Th(IV) from two kinds of carbon nano-materials and to evaluate their behavior in the environment. However, new detection method need to be developed for testing the adsorption of $C_{60}(OH)_n$ and $C_{60}(C(COOH)_2)_n$ on oMWCNTs. Further systematic investigation is needed to understand fully the sorption mechanism. Such studies are continuing and will be the subject of future articles.

Acknowledgments

Conflict of Interest

The authors declare no conflict of interest.

Appendix

Figure A1. Effect of $C_{60}(OH)_n$ and $C_{60}(C(COOH)_2)_n$ on the zeta potential of oMWCNTs. red line represent $C_{60}(OH)_n$ effect; blue line represent $C_{60}(C(COOH)_2)_n$ effect.
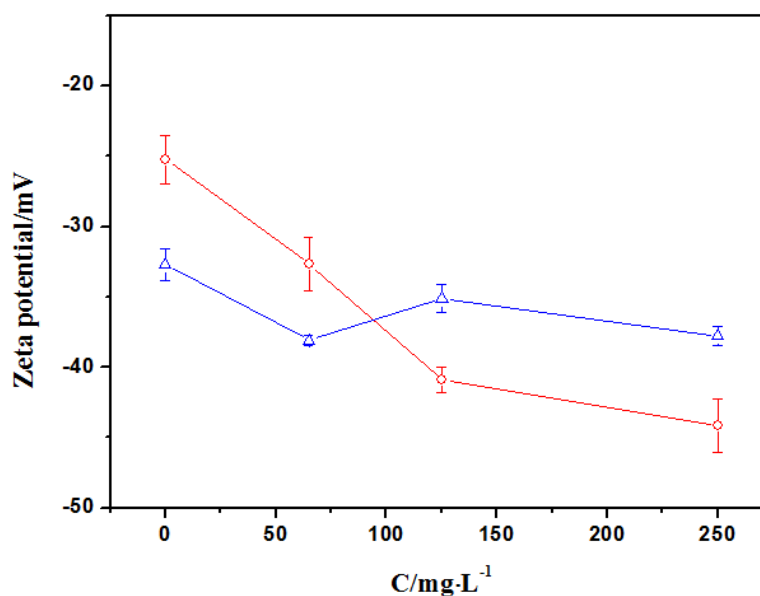
References

1. Balasubramanian, K.; Burghard, M. Chemically Functionalized Carbon Nanotubes. *Small* **2005**, *1*, 180–192.
2. Datsyuk, V.; Kalyva, M.; Papagelis, K.; Parthenios, J.; Tasis, D.; Siokou, A.; Kallitsis, I.; Galiotis, C. Chemical oxidation of multiwalled carbon nanotubes. *Carbon* **2008**, *46*, 833–840.
3. Hilding, J.; Grulke, E.A.; Zhang, Z.G.; Lockwood, F. Dispersion of carbon nanotubes in liquids. *J. Disper. Sci. Technol.* **2003**, *24*, 1–41.

4. Hussain, C.M.; Saridara, C.; Mitra, S. Microtrapping characteristics of single and multi-walled carbon nanotubes. *J. Chromatogr. A* **2008**, *1185*, 161–166.

5. Chen, C.; Li, X.; Zhao, D.; Tan, X.; Wang, X. Adsorption kinetic, thermodynamic and desorption studies of Th(IV) on oxidized multi-wall carbon nanotubes. *Colloids Surf. A Physicochem. Eng. Asp.* **2007**, *302*, 449–454.

6. Wang, X.; Chen, C.; Hu, W.; Ding, A.; Xu, D.; Zhou, X. Sorption of [243]Am(III) to Multiwall Carbon Nanotubes. *Environ. Sci. Technol.* **2005**, *39*, 2856–2860.

7. Chen, C.; Hu, J.; Xu, D.; Tan, X.; Meng, Y.; Wang, X. Surface complexation modeling of Sr(II) and Eu(III) adsorption onto oxidized multiwall carbon nanotubes. *J. Colloid Interf. Sci.* **2008**, *323*, 33–41.

8. Nowack, B.; Bucheli, T.D. Occurrence, behavior and effects of nanoparticles in the environment. *Environ. Pollut.* **2007**, *150*, 5–22.

9. Davoren, M.; Herzog, E.; Casey, A.; Cottineau, B.; Chambers, G.; Byrne, H.J.; Lyng, F.M. *In vitro* toxicity evaluation of single walled carbon nanotubes on human A549 lung cells. *Toxicol Vitro* **2007**, *21*, 438–448.

10. Simon-Deckers, A.; Gouget, B.; Mayne-L'Hermite, M.; Herlin-Boime, N.; Reynaud, C.; Carrière, M. *In vitro* investigation of oxide nanoparticle and carbon nanotube toxicity and intracellular accumulation in A 549 human pneumocytes. *Toxicology* **2008**, *253*, 137–146.

11. Fan, Q.H.; Shao, D.D.; Hu, J.; Chen, C.; Wu, W.; Wang, X. Adsorption of humic acid and Eu (III) to multi-walled carbon nanotubes: Effect of pH, ionic strength and counterion effect. *Radiochim. Acta* **2009**, *97*, 141–148.

12. Raju, C.S.K.; Subramanian, M. DAPPA grafted polymer: an efficient solid phase extractant for U (VI), Th (IV) and La (III) from acidic waste streams and environmental samples. *Talanta* **2005**, *67*, 81–89.

13. Jain, V.; Pandya, R.; Pillai, S.; Shrivastav, P. Simultaneous preconcentration of uranium (VI) and thorium (IV) from aqueous solutions using a chelating calix[4]arene anchored chloromethylated polystyrene solid phase. *Talanta* **2006**, *70*, 257–266.

14. Aydin, F.A.; Soylak, M. Solid phase extraction and preconcentration of uranium(VI) and thorium(IV) on Duolite XAD761 prior to their inductively coupled plasma mass spectrometric determination. *Talanta* **2007**, *72*, 187–192.

15. Benkhedda, K.; Epov, V.N.; Evans, R.D. Flow-injection technique for determination of uranium and thorium isotopes in urine by inductively coupled plasma mass spectrometry. *Anal. Bioanal. Chem.* **2005**, *381*, 1596–1603.

16. Östhols, E.; Manceau, A.; Farges, F.; Charlet, L. Adsorption of Thorium on Amorphous Silica: An EXAFS Study. *J. Colloid Interf. Sci.* **1997**, *194*, 10–21.

17. Chen, C.L.; Wang, X.K. Influence of pH, soil humic/fulvic acid, ionic strength and foreign ions on sorption of thorium(IV) onto γ-Al_2O_3. *Appl. Geochem.* **2007**, *22*, 436–445.

18. Zuo, L.; Yu, S.; Zhou, H.; Tian, X.; Jiang, J. Th(IV) adsorption on mesoporous molecular sieves: effects of contact time, solid content, pH, ionic strength, foreign ions and temperature. *J. Radioanal. Nucl. Chem.* **2011**, *288*, 379–387.

19. Bursali, E.A.; Merdivan, M.; Yurdakoc, M. Preconcentration of uranium (VI) and thorium (IV) from aqueous solutions using low-cost abundantly available sorbent. *J. Radioanal. Nucl. Chem.*

2010, *283*, 471–476.

20. Chen, C.L.; Wang, X.K.; Nagatsu, M. Europium Adsorption on Multiwall Carbon Nanotube/Iron Oxide Magnetic Composite in the Presence of Polyacrylic Acid. *Environ. Sci. Technol.* **2009**, *43*, 2362–2367.

21. Sun, Y.; Yang, S.; Sheng, G.; Guo, Z.; Wang, X. The removal of U(VI) from aqueous solution by oxidized multiwalled carbon nanotubes. *J. Environ. Radioactiv.* **2012**, *105*, 40–47.

22. Bühl, M.; Hirsch, A. Spherical aromaticity of fullerenes. *Chem. Rev.* **2001**, *101*, 1153–1183.

23. Montes-Morán, M.A.; Suárez, D.; Menéndez, J.A.; Fuente, E. On the nature of basic sites on carbon surfaces: an overview. *Carbon* **2004**, *42*, 1219–1225.

24. Avilés, F.; Cauich-Rodríguez, J.V.; Moo-Tah, L.; May-Pat, A.; Vargas-Coronado, R. Evaluation of mild acid oxidation treatments for MWCNT functionalization. *Carbon* **2009**, *47*, 2970–2975.

25. Lu, C.; Liu, C.; Rao, G.P. Comparisons of sorbent cost for the removal of Ni^{2+} from aqueous solution by carbon nanotubes and granular activated carbon. *J. Hazard Mater.* **2008**, *151*, 239–246.

26. Xu, J.Y.; Han, K.; Li, S.X.; Cheng, J.S.; Xu, G.T.; Li, W.X.; Li, Q.N. Pulmonary responses to polyhydroxylated fullerenols, $C_{60}(OH)_x$. *J. Appl. Toxicol.* **2009**, *29*, 578–584.

27. Cheng, F.; Yang, X.; Zhu, H.; Sun, J.; Liu, Y. Synthesis of oligoadducts of malonic acid C_{60} and their scavenging effects on hydroxyl radical. *J. Phys. Chem. Solids* **2000**, *61*, 1145–1148.

28. Ren, X.; Wang, S.; Yang, S.; Li, J. Influence of contact time, pH, soil humic/fulvic acids, ionic strength and temperature on sorption of U(VI) onto MX-80 bentonite. *J. Radioanal. Nucl. Chem.* **2010**, *283*, 253–259.

29. Ho, Y.S. Adsorption of heavy metals from waste streams by peat. Ph.D. Dissertation, The University of Birmingham, Birmingham, UK, 1995.

30. Tan, X.; Wang, X.; Fang, M.; Chen, C. Sorption and desorption of Th(IV) on nanoparticles of anatase studied by batch and spectroscopy methods. *Colloids Surf. A Physicochem. Eng. Aspects* **2007**, *296*, 109–116.

31. Chen, C.; Wang, X. Sorption of Th (IV) to silica as a function of pH, humic/fulvic acid, ionic strength, electrolyte type. *Appl. Radiat. Isotopes* **2007**, *65*, 155–163.

32. Zhao, D.; Sheng, G.; Hu, J.; Chen, C.; Wang, X. The adsorption of Pb(II) on Mg_2Al layered double hydroxide. *Chem. Eng. J.* **2011**, *171*, 167–174.

33. Sheng, G.; Li, J.; Shao, D.; Hu, J.; Chen, C.; Chen, Y.; Wang, X. Adsorption of copper(II) on multiwalled carbon nanotubes in the absence and presence of humic or fulvic acids. *J. Hazard Mater.* **2010**, *178*, 333–340.

34. Tan, X.; Wang, X.; Chen, C.; Sun, A. Effect of soil humic and fulvic acids, pH and ionic strength on Th(IV) sorption to TiO_2 nanoparticles. *Appl. Radiat. Isotopes* **2007**, *65*, 375–381.

35. Choppin, G. Actinide speciation in the environment. *J. Radioanal. Nucl. Chem.* **2007**, *273*, 695–703.

36. Anirudhan, T.S.; Rijith, S.; Tharun, A.R. Adsorptive removal of thorium(IV) from aqueous solutions using poly(methacrylic acid)-grafted chitosan/bentonite composite matrix: Process design and equilibrium studies. *Colloids Surf. A Physicochem. Eng. Aspects* **2010**, *368*, 13–22.

37. Sheng, G.; Hu, J.; Wang, X. Sorption properties of Th(IV) on the raw diatomite—Effects of contact time, pH, ionic strength and temperature. *Appl. Radiat. Isotopes* **2008**, *66*, 1313–1320.

38. Yang, S.; Li, J.; Lu, Y.; Chen, Y.; Wang, X. Sorption of Ni(II) on GMZ bentonite: Effects of pH, ionic strength, foreign ions, humic acid and temperature. *Appl. Radiat. Isotopes* **2009**, *67*, 1600–1608.

39. Yu, S.; Ren, A.; Cheng, J.; Song, X.; Chen, C.; Wang, X. Comparative study on sorption of radiocobalt to montmorillonite and its Al-pillared and cross-linked samples: Effect of pH, ionic strength and fulvic acid. *J. Radioanal. Nucl. Chem.* **2007**, *273*, 129–133.

40. Bradbury, M.; Baeyens, B. Sorption of Eu on Na-and Ca-montmorillonites: Experimental investigations and modelling with cation exchange and surface complexation. *Geochim. Cosmochim. Ac.* **2002**, *66*, 2325–2334.

41. Wang, X.; Liu, X. Sorption and desorption of radioselenium on calcareous soil and its solid components studied by batch and column experiments. *Appl. Radiat. Isotopes* **2005**, *62*, 1–9.

42. Wu, W.; Fan, Q.; Xu, J.; Niu, Z.; Lu, S. Sorption-desorption of Th(IV) on attapulgite: Effects of pH, ionic strength and temperature. *Appl. Radiat. Isotopes* **2007**, *65*, 1108–1114.

43. Talip, Z.; Eral, M.; Hiçsönmez, Ü. Adsorption of thorium from aqueous solutions by perlite. *J. Environ. Radioactiv.* **2009**, *100*, 139–143.

44. Reiller, P.; Moulin, V.; Casanova, F.; Dautel, C. Retention behaviour of humic substances onto mineral surfaces and consequences upon thorium (IV) mobility: case of iron oxides. *Appl. Geochem.* **2002**, *17*, 1551–1562.

45. Zhijun, G.; Lijun, N.; Zuyi, T. Sorption of Th(IV) ions onto TiO_2: Effects of contact time, ionic strength, thorium concentration and phosphate. *J. Radioanal. Nucl. Chem.* **2005**, *266*, 333–338.

46. Yu, S.M.; Chen, C.L.; Chang, P.P.; Wang, T.T.; Lu, S.S.; Wang, X.K. Adsorption of Th(IV) onto Al-pillared rectorite: Effect of pH, ionic strength, temperature, soil humic acid and fulvic acid. *Appl. Clay. Sci.* **2008**, *38*, 219–226.

47. Chen, W.; Duan, L.; Wang, L.; Zhu, D. Adsorption of Hydroxyl- and Amino-Substituted Aromatics to Carbon Nanotubes. *Environ. Sci. Technol.* **2008**, *42*, 6862–6868.

48. Yang, S.T.; Guo, W.; Lin, Y.; Deng, X.Y.; Wang, H.F.; Sun, H.F.; Liu, Y.F.; Wang, X.; Wang, W.; Chen, M.; *et al.* Biodistribution of Pristine Single-Walled Carbon Nanotubes *in Vivo*. *J. Phys. Chem. C* **2007**, *111*, 17761–17764.

49. Chen, W.; Duan, L.; Zhu, D. Adsorption of Polar and Nonpolar Organic Chemicals to Carbon Nanotubes. *Environ. Sci. Technol.* **2007**, *41*, 8295–8300.

50. Li, T.; Li, X.; Huang, K.; Jiang, H.; Li, J. Synthesis and characterization of hydroxylated fullerene epoxide—An intermediate for forming fullerol. *J. Cent. South Univ. T* **1999**, *6*, 35–36.

51. Ye, C.; Chen, C.; Chen, Z.; Meng, H.; Xing, L.; Jiang, Y.; Yuan, H.; Xing, G.; Zhao, F.; Zhao, Y. *et al. In situ* observation of $C_{60}(C(COOH)_2)_2$ interacting with living cells using fluorescence microscopy. *Chin. Sci. Bull* **2006**, *51*, 1060–1064.